Journal of Electrical and Computer Engineering Innovations
(JECEI)
Journal homepage: http://www.jecei.sru.ac.ir

Research paper

Modelling and Optimization of Channel Allocation for Power Line Communications Access Networks in the Presence of In-Line and In-Space Interference

***M. Sheikh-Hosseini*[1, *], *S.M. Nosratabadi*[2]**

[1]*Department of Computer and Information Technology, Institute of Science and High Technology and Environmental Sciences, Graduate University of Advanced Technology, Kerman, Iran.*

[2]*Department of Electrical Engineering, Sirjan University of Technology, Sirjan, Iran.*

Article Info

Article History:
Received 26 April 2020
Reviewed 27 June 2020
Revised 22 July 2020
Accepted 23 November 2020

Keywords:
Broadband power line communications (B-PLC) access network
PLC channel allocation (PLC-CA) problem
In-line and in-space neighboring schemes
Co-site interference
Genetic and Shuffled frog-leaping algorithms

*Corresponding Author's Email Address:
m.sheikhhosseini@kgut.ac.ir

Abstract

Background and Objectives: Broadband power line communications (PLC) is a promising candidate for implementing access network of different telecommunication Technologies. Planning process of the PLC access network is subdivided into two main optimization problems of the generalized base station placement and PLC channel allocation.

Methods: This paper studies the latter one for an actual PLC network by taking both in-line and in-space neighboring schemes into account for the first time and modeling the PLC channel allocation according to them. In this regards, different aspects of this problem are first introduced in details and then our suggested models for them are presented and numerically evaluated.

Results: Specifically, for each pair of the broadband-PLC cells, in-line neighboring is modeled either by one or zero indicating the cells are neighbor or not; in-space neighboring is suggested to be a number from the interval [0 1] according to physical vicinity of cell's wirings; and consequently aggregate neighboring intensity will be a number from [0 2]. Subsequently, the network interference is defined as a function of neighboring intensity and assigned frequency sets to the neighbor cells; so that the more neighboring intensity is increased and the more distance between the sets is decreased, the more interference is imposed on the PLC network. Eventually, the meta-heuristic methods of Genetic and shuffled frog-leaping algorithms are exploited to solve resulting PLC channel allocation problem via minimizing the interference.

Conclusion: In general, the results confirmed the success of the suggested method in modeling PLC channel allocation problem in actual scenarios, tracking the network interference in these situations, providing an optimal solution for them, and including all previous research as a comprehensive method.

Introduction

Power Line Communications (PLC) technology utilizes existing electrical infrastructure to provide and deliver various telecommunications services. History of this technology dates back to the 1900's, and its fast and low-cost deployment together with the wide spread availability of power grids has been the most promoting factors encouraging power companies to develop PLC technology over the years [1]-[3]. Compared with other wireline technologies like fiber optic and coaxial cables, PLC has lower deployment cost, fast installation time and much more pervasive structure [4], [5]. Furthermore, since PLC utilizing already implemented infrastructure, its deployment cost is comparable with that one of wireless technologies [4], [5]. Moreover, to increase coverage and enable signal propagation through concrete walls in different floors, ultra-wideband PLC has been suggested as an alternative for the existing in-building wireless solutions [6], [7].

Different PLC technologies can be classified into three main categories of ultra-narrowband PLC (UN-PLC), narrowband-PLC (N-PLC) and broadband-PLC (B-PLC), where the ultra-narrowband and narrowband ones use frequency bands below 500 kHz and support date rates between a few hundreds of bits per second (b/s) up to a few Mb/s. However, the operation frequencies of B-PLC systems are more than 1 MHz and may reach to 250 MHz. B-PLC systems provide data rate ranging from several Mb/s to several hundred Mb/s [4], [5], [8]. PLC technology has wide application area including from management and monitoring tasks for power utilities, smart grid applications, implementing access network of different telecommunication systems as a last mile solution, to smart homing, in-home and in-building networking, and in-vehicle communications [9]-[11].

In the last two decades, PLC have also received increasing attention as a promising solutions for telecommunication infrastructure needed by smart grid and a new subcategory, called high data rate N-PLC, has been emerged and standardized by the PRIME, G3-PLC, IEEE and ITU-T alliances for applications such as automatic meter reading, vehicle-to-grid communications and networking of consumer appliances [12], [13]. Furthermore, it is worth to be noted that the integration of the PLC with wireless technologies such as radio frequency and visible light communications systems have also received great attention and explored to enhance performance metrics like coverage and reliability [14], [15].

However, power lines are very harsh medium and suffer from some constraints such as deep attenuation, multipath propagation and impulsive noise [16], [17]. To overcome them, orthogonal frequency division multiplexing (OFDM) has been received increasing interest as an anti-multipath technique [18] and adapted to the B-PLC and high data rate N-PLC standards [17].

As outlined earlier, B-PLC can be exploited to implement the last mile (or access network) of various telecommunication technologies. In a B-PLC access network, the low voltage grid is subdivided into several cells and these cells are equipped with PLC base stations (BS), modems and repeaters to establish connection of telecommunications backbone network with end-user subscribers via an OFDM-based system. Typical structure of a B-PLC access network is conceptually illustrated in Fig. 1, in which the cell's areas are distinguished by dotted lines and the BS terminal of each cell is located in the low voltage transformer station or a street cabinet. A more detailed structure of a typical B-PLC cell is shown in Fig. 2, where the BS terminal will connect the telecommunications backbone network to low voltage grid through an access point. At low voltage side, PLC modems over power outlets are utilized to connect the end-user devices to the BS terminal and the backbone network. In addition, several repeaters may be used in each cell to provide BS coverage for all users. As a result, this design enables injection of telecommunication signals into the low voltage grid and extraction of them from the grid. Planning process of B-PLC access network can be subdivided into two different optimization problems: the generalized base station placement (GBSP) problem and the PLC channel allocation (PLC-CA) problem [19]. The main task of former one is to optimize network cost and quality of service by determining the optimum number of cells for serving all users, the most appropriate locations of the BS terminals, the set of required repeaters and subset of users must be served by each cell or BS terminal. When GBSP problem is solved, the PLC-CA problem will rise to optimally share the PLC resources such as available OFDM frequencies between different B-PLC cells. Expressing with more details, in order to increase network capacity, the frequency reuse technique is used to assign bandwidth to different cells and this results in assignment of same or near frequencies to neighbor cells and imposing co-site interference on the B-PLC network. PLC-CA solution must manage this challenge by providing a channel allocation which keeps this interference at authorized level.

A. Related Works and Our Motivations

As outlined, design of the B-PLC access network has been first addressed in [19] by converting this process into problems of the GBPS and PLC-CA. This work was paved the way for subsequent research on these problems. In the case of the GBPS problem, this challenge has been modeled as an optimization problem in [20]-[22] and solved by minimizing the network costs and delay. The challenge of PLC-CA is first addressed in [23], [24], and modeled as an optimization problem. Subsequently, the authors have generalized their works in [23], [24] and investigating PLC-CA problem more precisely in [25]. Furthermore, it is worth to be noted that dynamic resource allocation, by assuming dynamic structure for the B-PLC cells, has been developed to the B-PLC access networks in [26].

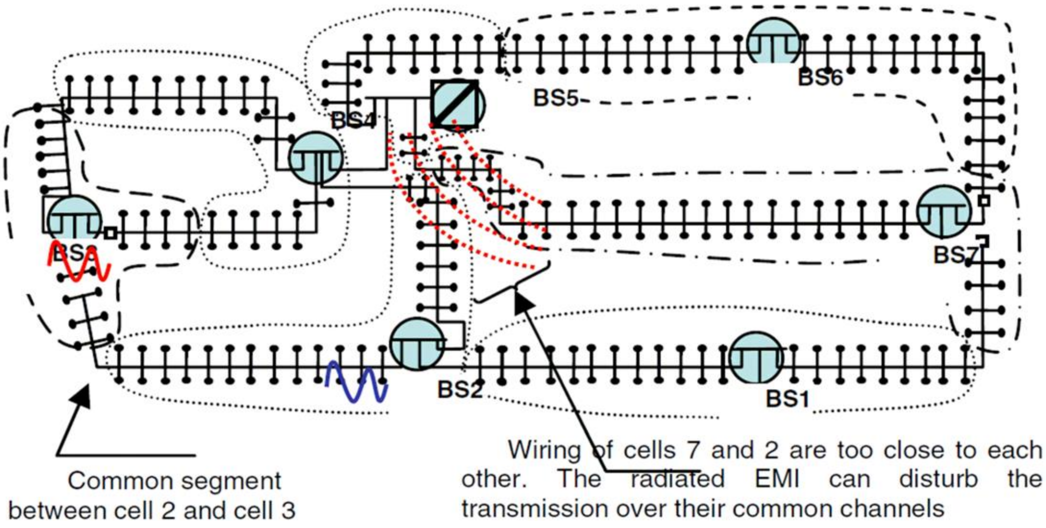

Fig. 1: Typical structure of a B-PLC access network [23].

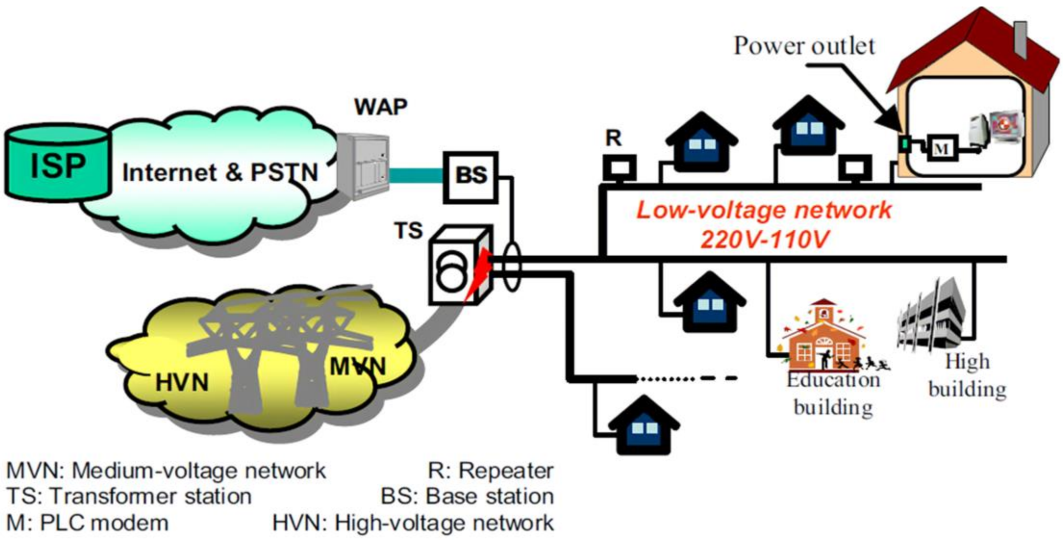

Fig. 2: Typical structure of a B-PLC cell [20].

However, similar to that one of [23]-[25], we investigate the channel allocation for the fixed B-PLC network and dynamic resource allocation falls beyond its scope.

Unfortunately, the provided analysis in [23]-[25] suffers from some limitations, since these works directly applied existing wireless solutions to the B-PLC networks without considering the differences between them. Expressing with more details, whereas there exist some similarities between B-PLC and wireless access networks, but the physical medium, size, geometrical shape and neighboring schemes of the cells are different in wireless and PLC networks.

In fact, PLC uses a physical medium with a specific wiring topology, and the PLC cells (as demonstrated in Fig. 2) are not similar to that one's of the wireless networks, i.e. hexagonal cells in free space. More specifically, in contrast to wireless, there exist two different neighboring schemes for the B-PLC access networks. These are in-line and in-space neighboring. In-line neighboring is due to existence of common segments or wirings between two cells and generates conducted disturbances in the form of electrical signal. However, in-space neighboring is due to physical vicinity of wirings and generates disturbances in the term of electromagnetic signals. For instance, as demonstrated in Fig. 1, the cells 3 and 7 are in-line and in-space neighbors of the cell 2, respectively. Thereby, the channel and resource allocation in wireless scenarios (like [27] and [28]) is different from that one of the B-PLC networks and these are two distinct problems needing different models, analyses and solutions.

However, these differences have not taken into account in [23]-[25] and they have considered the B-PLC network similar to a wireless environment, which is only in expose of the in-line neighboring scheme.

Consequently, the PLC-CA have been modeled and analyzed in this regard and the impact of co-site interference imposed by in-space neighboring scheme has been ignored. This is while in-space neighboring is the main distinguishing feature of the PLC access and wireless networks. Therefore, it is necessary and vital to investigate and analyze the PLC-CA problem for the actual B-PLC networks by taking these differences into account. The lacks of this analysis has motivated us to devote this research on investigation of the PLC-CA problem over actual networks by taking both in-line and in-space neighboring schemes into account.

B. Our Contributions and Paper Organization

In order to overcome the above-mentioned limitations, this paper is devoted to investigating PLC-CA problem for the actual B-PLC access network by taking both in-line and in-space neighboring schemes into account and allocating channels accordingly. In this regard, in-line neighboring is modeled either by one or zero similar to [23]-[25]; however, in-space neighboring is considered as a real number from the interval [0 1] according to physical vicinity of cell's wirings; and the aggregate neighboring intensity is assumed as the summation of these two numbers. Then, the co-site interference of the B-PLC access networks is defined as a function of the aggregate neighboring intensity and the assigned frequency sets to the cells, so that the interference is increased when the value of neighboring intensity is increased and the distance of assigned frequency sets is decreased. Finally, the resulting co-site interference is minimized using genetic algorithm (GA) and shuffled frog-leaping algorithm (SFLA), and the assigned channels to cells are extracted. In general, the suggested method has advantage over the existing studies in terms of considering actual PLC network, providing more suitable and accurate model for the co-site interference, and evaluating the performance using two evolutionary methods and various realizations. However, since providing full details requires the problem model and its formulation and parameters, our contributions and novelties and their modifications over existing works have been postponed until the second part of the next section and highlighted in details at the beginning of this part.

The rest of paper is organized as follows: In Section II, we present the main results of this study by modeling PLC-CA problem as an optimization problem and suggesting our models for neighboring schemes and co-site interference. Optimum performance of these models is numerically evaluated and verified in Section III. Finally, Section VI includes conclusion.

Notations: Throughout this paper, matrices are defined by boldface letters like $\boldsymbol{M}$, where m_{ij} indicates its (i,j) element. The notations $\mathcal{A}$ are used to define sets, where $|\mathcal{A}|$ indicates the set cardinality, i.e. the number of elements in the sets.

Main Results

In this section, the PLC-CA problem is first formalized as an optimization problem and then the suggested models for different aspects of this problem are presented.

C. Modeling PLC-CA Problem as an Optimization Problem

Generally speaking, planning process of B-PLC access network includes dividing the low voltage power gird into several cells; equipping each cell with a BS terminal, PLC modems and repeaters; determining the subset of users have to be served by each cell; and assigning OFDM channels (frequencies) needed by each cell to serve its users.

In this paper, available B-PLC cells and OFDM frequencies are denoted by the sets $\mathcal{C} = \{\mathcal{C}_1, \mathcal{C}_2, \dots, \mathcal{C}_{|\mathcal{C}|}\}$ and $\mathcal{F}_s = \{\mathcal{F}_1, \mathcal{F}_2, \dots, |\mathcal{F}_s|\}$ respectively, where $|\mathcal{C}|$ and $|\mathcal{F}_s|$ are the cardinality of these sets. The i^{th} cell, i.e. $\mathcal{C}_i$, is modeled by $\mathcal{C}_i = \{B_i, \mathcal{U}_s^i, \mathcal{R}_s^i, \mathcal{F}_{CA}^i\}$, where B_i indicates to BS terminal and its access point, $\mathcal{R}_s^i$ determines its repeaters set and $\mathcal{U}_s^i$ represents the subset of users have to be served by this cell. These three quantities, i.e. B_i, $\mathcal{R}_s^i$ and $\mathcal{U}_s^i$, are determined by solving the GBSP problem and the task of PLC-CA is to discover $\mathcal{F}_{CA}^i$, where $\mathcal{F}_{CA}^i$ represents the set of assigned frequencies to cell $\mathcal{C}_i$.

In general, any solution of the PLC-CA problem can be represented using a binary matrix of size $|\mathcal{C}| \times |\mathcal{F}_s|$. Throughout this paper, we have named this matrix by $\boldsymbol{M}^{CA}$, where $m_{ij}^{CA} = 1$ means that the j^{th} frequency of the $\mathcal{F}_s$ has been assigned to the cell $\mathcal{C}_i$ and $m_{ij}^{CA} = 0$ means this frequency has not allocated to this cell. Note that the index values of non-zero elements in i^{th} row of $\boldsymbol{M}^{CA}$ are the members of assigned frequency set to cell $\mathcal{C}_i$, i.e. $\mathcal{F}_{CA}^i$.

The requirements and constraints must be taken into account for solving PLC-CA problem are as below:

- First, due to some technical and regulatory restrictions, cell $\mathcal{C}_i$ may has a forbidden frequency set as $\mathcal{F}_{Forbid}^i$. Thus, its allowable frequency set is $\mathcal{F}^i = \mathcal{F}_s - \mathcal{F}_{Forbid}^i$, and the constraint of $\mathcal{F}_{CA}^i \subseteq \mathcal{F}^i$ must be met in solving PLC-CA problem.
- To guarantee serving of all users, the number of assigned frequencies to cell $\mathcal{C}_i$ must be as $|F_{Req}^i| = A_{User}|U_s^i|$, where $|U_s^i|$ is the number of allocated users to this cell and A_{User} is a constant number representing the average number of frequencies needed by each user to provide the traffic requested in its downlink and uplink channels. This imposes another constraint to the PLC-CA problem as

$|\mathcal{F}_{CA}^{i}| \geq |F_{Req}^{i}|$.

- Moreover, to optimally solve PLC-CA problem, it is necessary to minimize the co-site interference. Since the in-line and in-space neighboring are the sources of the co-site interference over B-PLC access networks, PLC-CA solution must keep the summation of these two interferences at authorized level by increasing distance between assigned frequencies to neighbor cells as much as possible. Hence, a $|\mathcal{C}| \times |\mathcal{C}|$ matrix, called interference distance matrix $\boldsymbol{M}^{ID}$, is needed to determine the threshold limits of interference for each pair of cells. Indeed, elements of this matrix are the thresholds determining assigned frequencies to cells leading to co-site interference or not. Expressing more precisely, for the two neighbor cells of $\mathcal{C}_i$ and $\mathcal{C}_{i'}$, if distance between the frequency f_i of $\mathcal{C}_i$ and $f_{i'}$ of $\mathcal{C}_{i'}$ is less than $m_{ii'}^{ID}$, i.e. $|f_i - f_{i'}| < m_{ii'}^{ID}$, then this assignment of frequency leads to network interference. But, when $|f_i - f_{i'}| \geq m_{ii'}^{ID}$, this assignment has no interference effect on the network.

According to the above considerations, the PLC-CA problem can be generally formalized as a combinatorial optimization problem with the following specifications:

- Inputs:

1. The output of GBSP problem, which is the set of cells $\mathcal{C} = \{\mathcal{C}_1, \mathcal{C}_2, \dots, \mathcal{C}_{|\mathcal{C}|}\}$ with their details of $\{B_i, \mathcal{U}_s^i, \mathcal{R}_s^i\}$.
2. The sets $\mathcal{F}_s$ and $\mathcal{F}_{Forbid}^{i}$, to compute $\mathcal{F}^i = \mathcal{F}_s - \mathcal{F}_{Forbid}^{i}$ for the cells.
3. The interference distance matrix $\boldsymbol{M}^{ID}$.
4. The aggregate neighborhood matrix $\boldsymbol{M}^{NB}$ which is summation of in-line and in-space neighboring matrices.
5. The average number of frequencies needed by each cell, i.e. A_{User}, to compute $|F_{Req}^{i}| = A_{User}|U_s^i|$ for each cell.

- Output:

1. The solution matrix $\boldsymbol{M}^{CA}$, to extract the assigned frequency sets of different B-PLC cells, i.e. $\mathcal{F}_{CA}^{i}$ for $i = 1,2,\dots,|\mathcal{C}|$.

- Objectives:

1. Minimization of the co-site interference of the B-PLC access network.

- Constraints:

1. $\mathcal{F}_{CA}^{i} \subseteq \mathcal{F}^i$
2. $|F_{Req}^{i}| \leq |\mathcal{F}_{CA}^{i}| \leq |\mathcal{F}^i|$

D. Suggested Models for the Different Aspects of the PLC-CA Problem

In the sequel, our proposed methods for the modeling of neighboring schemes, co-site interference and interference distance matrix are provided in a respective order. Compared with the existing study of [23]-[25], the contributions and novelties of our research can be highlighted as:

- In [23]-[25], in-line neighboring scheme has only considered for the B-PLC access networks and for each pair of B-PLC cells, the neighboring is modeled either by zero or one. However, we investigate PLC-CA problem for an actual PLC network in the presence of both in-line and in-space neighboring schemes. Since the binary model of [23]-[25] has no longer holds, we suggest a fuzzy model where the aggregate neighboring intensity for each cell pair will be real number from the interval [0 2].
- In [23]-[25], elements of interference distance matrix $\boldsymbol{M}^{ID}$ are considered equal to a constant number. In our study, these elements are intelligently defined as a function of aggregate neighboring intensity of the cells. As it will be described later, this definition makes solver of PLC-CA problem more sensitive to cells having greater neighboring intensity and increases the distance between assigned frequency sets to them.
- In [23]-[25], the amount of co-site interference imposed on network by different neighbor cells are considered equal to each other's. Here, as a more appropriate and efficient model, the co-site interference is defined as a function of neighboring intensity of the B-PLC cells and the assigned frequency sets to them. According to this, for each pair of neighbor cells, the more neighboring intensity is increased and the more distance between assigned frequency sets is decreased, the more interference is imposed on network.
- It is also worth to be noted that a general formulation is provided for the co-site interference which subsumes many realizations such as existing ones of [23]-[25].
- In addition to the GA, SFLA are also utilized to verify the optimum performance of the suggested models for different realizations of interference function, neighboring models and forbidden sets.

I) Formulation of the Neighboring Schemes

The proposed models for in-line, in-space and aggregate neighboring schemes can be summarized as follows:

- Similar to [23]-[25]., in-line neighboring is modeled by a $|\mathcal{C}| \times |\mathcal{C}|$ binary matrix, whose entries are zero or one. Here, this matrix is denoted by $\boldsymbol{M}^{NB_L}$, where $m_{ii'}^{NB_L} = 1$ implies to in-line neighboring of cells $\mathcal{C}_i$ and $\mathcal{C}_{i'}$, and $m_{ii'}^{NB_L} = 0$ indicates these cells are not in-line neighbor.
- Since in-space neighboring is due to physical vicinity of cell's wirings and its strength changes according to the degree of this vicinity, it is modeled by a fuzzy

approach and the elements of $|\mathcal{C}| \times |\mathcal{C}|$ in-space neighboring matrix of $\boldsymbol{M}^{NB_S}$ are chosen from the interval [0 1]. In this manner, $m_{ii'}^{NB_S} = 0$ indicates cells C_i and $C_{i'}$ are not in-space neighbor; however, if these cells are in-space neighbor, then the value of $m_{ii'}^{NB_S}$ will be a non-zero number from (0 1]. Note that the amount of $m_{ii'}^{NB_S}$ directly depends on the vicinity degree of cell's wirings and the more physical vicinity of wirings is increased, $m_{ii'}^{NB_S}$ is more increased until reaches its upper limit equal to one, which is equivalent to in-line neighboring.

- Eventually, the aggregate neighboring is defined by $\boldsymbol{M}^{NB} = \boldsymbol{M}^{NB_L} + \boldsymbol{M}^{NB_S}$, which is a $|\mathcal{C}| \times |\mathcal{C}|$ matrix whose elements belonging to interval [0 2] indicating the neighboring intensity of the different B-PLC cells.

Note that since the cells are not the neighbor of themselves, the main diagonal elements of matrices $\boldsymbol{M}^{NB_L}$, $\boldsymbol{M}^{NB_S}$ and $\boldsymbol{M}^{NB}$ are always equal to zero.

II) Formulation of the Co-Site Interference

In this part, we present our proposed models for the co-site interference and interference distance matrix. In order to provide more insight, the function of co-site interference is first formalized for the two B-PLC cells of C_i and $C_{i'}$, and then generalized to the whole network.

The co-site interference generated between the cells C_i and $C_{i'}$ or imposed on network by the cells C_i and $C_{i'}$ can be formalized as follows:

$$I_{ii'}\left(F, m_{ii'}^{NB}\right) = \begin{cases} \sum_{f \in \mathcal{F}_{CA}^{i}} \sum_{f' \in \mathcal{F}_{CA}^{i'}} G_1\left(F, m_{ii'}^{NB}\right) & F \le m_{ii'}^{ID} \\ 0 & F > m_{ii'}^{ID} \end{cases} \tag{1}$$

in which $I_{ii'}$ represents the co-site interference imposed on network by the cells C_i and $C_{i'}$. $\mathcal{F}_{CA}^{i}$ and $\mathcal{F}_{CA}^{i'}$ are the assigned frequency sets to the cells C_i and $C_{i'}$ respectively. $F = |f_i - f_{i'}|$ is the distance between members of these sets, $m_{ii'}^{ID}$ represents the (i, i') element of interference distance matrix $\boldsymbol{M}^{ID}$, and the function of $G_1\left(F, m_{ii'}^{NB}\right)$ indicates to the co-site interference for the specific values of F and $m_{ii'}^{NB}$.

As outlined earlier, $m_{ii'}^{ID}$ denotes a threshold value determining assigned frequencies to the cells C_i and $C_{i'}$ leading to co-site interference or not. As described below, to properly model interference distance matrix, we define this threshold as a function of neighboring intensity using $m_{ii'}^{ID} = G_2\left(m_{ii'}^{NB}\right)$.

The continuous functions of $G_1(F, x)$ and $G_2(x)$ must meet following necessary conditions:

- First of all, since co-site interference does not generate by non-neighbor cells, $I_{ii'}$ must be equal to zero for any $m_{ii'}^{Neigh} = 0$. Consequently, $G_1(F, x)$ must be such that $G_1(F, x)|_{x=0} = 0$.
- Since the amplitude of the co-site interference directly depends on the $G_1(F, x)$, this function must be such that (i): the more neighboring intensity is increased, the more co-site interference is imposed on network, (ii): the more distance between assigned frequency sets of neighbor cells is decreased, the more co-site interference is produced. Hence, $G_1(F, x)$ must be a strictly increasing function of the x and a strictly decreasing function of the F.
- In [23]-[25], the elements of the interference distance matrix $\boldsymbol{M}^{ID}$ are considered equal to a constant number. Here, to provide a more efficient model, these elements are defined as a strictly increasing function of neighboring intensity using $G_2\left(m_{ii'}^{NB}\right) = m_{ii'}^{ID}$. According to this model, if the neighboring intensity of the cells C_{i_1} and $C_{i_1'}$ being more than that of C_{i_2} and $C_{i_2'}$, i.e. $m_{i_1 i_1'}^{NB} > m_{i_2 i_2'}^{NB}$, then $m_{i_1 i_1'}^{ID} > m_{i_2 i_2'}^{ID}$. Thereby, more co-site interference will be counted using (1) for the cells C_{i_1} and $C_{i_1'}$ in comparison with that of C_{i_2} and $C_{i_2'}$. Consequently, the interference function is more sensitive to the cells having greater neighboring intensity and this finally increases the distance between assigned frequencies to these cells during the process of interference minimization.

In the following, these conditions are more clarified by considering some special realizations for the $G_1(F, x)$ and $G_2(x)$.

- $G_1(F, x) = a$ and $G_2(x) = b$, for any positive number of a and b: This realization does not satisfy the above-mentioned conditions and is actually similar to that one considered in [23]-[25]. Since dependency of interference function to neighboring intensity has been ignored in this realization, taking in-space neighboring into account has no impact on solution of the PLC-CA problem and the performance of this realization in the presence and the absence of in-space neighboring is identical and similar to that one reported in [23]-[25] for in-line neighboring.
- Realizations of the $G_1(F, x)$: Any continuous function satisfying the first two of above conditions will be a realization for $g_1(F, x)$, where $g_1(F, x) = \frac{x^2}{1 + \frac{F}{|\mathcal{F}_S|}}$ and $g_1(F, x) = (1 + x^2)e^{-\frac{F}{|\mathcal{F}_S|}}$ are the two examples that are included for the numerical simulations of next section.
- Realizations of the $G_2(x)$: Examples like $G_2(x) = x + |\mathcal{F}_S|$ and $G_2(x) = |\mathcal{F}_S| x$ are two realizations of $G_2(x)$ satisfying the last condition of above and also utilized for the numerical simulations.

Eventually, the whole co-site interference of the B-PLC access network is obtained from (1) by summation over all cells as:

$$I = \frac{1}{|\mathcal{C}||\mathcal{F}_s|} \sum_{i \in \mathcal{C}} \sum_{i' \in \mathcal{C}} I_{ii'} \tag{2}$$

in which $\mathcal{C} = \{\mathcal{C}_1, \mathcal{C}_2, \dots, \mathcal{C}_{|\mathcal{C}|}\}$ and $\mathcal{F}_s = \{\mathcal{F}_1, \mathcal{F}_2, \dots, |\mathcal{F}_s|\}$ are the sets of available B-PLC cells and the available OFDM frequencies with the cardinality of $|\mathcal{C}|$ and $|\mathcal{F}_s|$, respectively.

In the next section, the evolutionary algorithms are utilized to solve PLC-CA problem via minimizing this interference function.

Numerical Results and Discussion

This section is dedicated to the numerical results and analyzing the performance of the proposed model for the optimization problem of PLC-CA. In this regard, GA and SFLA, as two population-based meta-heuristic methods, are exploited and implemented using MATLAB software. It is worth to be noted that GA has been inspired from natural selection and corrects an initial random population in the consecutive iterations using operations like elitism, selection, crossover, mutation, until converging to the solution [29], [30]. In order to prevent convergence to local optima in some problems, new advanced algorithms like SFLA have been proposed, which inspired by the collective evolution of frogs in obtaining food supply and benefits from local search and information mixing in its evolution process to find the global optimum and prevent convergence to local optima [31]. It must be noted that since the PLC-CA problem is a combinatorial optimization problem, the binary versions of GA and SFLA are exploited to solve the PLC-CA problem and optimally discover the assigned frequency sets to the cells.

Performance of the suggested model is evaluated for two different B-PLC test networks, where the first one is consisted of three B-PLC cells and utilizes an OFDM modulation having ten frequencies; however, the second one relies on six B-PLC cells and employs OFDM modulation of 64 frequencies. In order to diversify the results and allow comparison with the previous studies, the experiments of each test network have been performed for the two different scenarios as detailed in Table 1. As can be seen from the Table 1, the first scenario investigates the performance in the absence of forbidden sets for the B-PLC cells; However, the second one takes the forbidden sets into account. Moreover, numerical simulations of each scenario have also been performed for the two different cases; case 1: which only considers in-line neighboring scheme similar to that one of previous studies in [23]-[25], and case 2: where takes both in-line and in-space neighboring schemes into account. Further, to provide a fair comparison in these two cases, the numerical simulations of them have also been performed for the identical interference functions of $G_1(F,x)$ and $G_2(x)$.

Table 1: Specifications of the considered scenarios for the performance evaluation of the B-PLC test networks

Scenario	Case	$\mathcal{F}^i_{Forbid}$	Interference Functions		Neighboring Matrices	
			G_1	G_2	$\boldsymbol{M}^{NB_L}$	$\boldsymbol{M}^{NB_S}$
First	1	No	$\frac{\lvert\mathcal{F}_s\rvert x^2}{F+\lvert\mathcal{F}_s\rvert}$	$x+\lvert\mathcal{F}_s\rvert$	Yes	No
	2	No	$\frac{\lvert\mathcal{F}_s\rvert x^2}{F+\lvert\mathcal{F}_s\rvert}$	$x+\lvert\mathcal{F}_s\rvert$	Yes	Yes
Second	1	Yes	$\frac{1+x^2}{e^{\frac{F}{\lvert\mathcal{F}_s\rvert}}}$	$\lvert\mathcal{F}_s\rvert x$	Yes	No
	2	Yes	$\frac{1+x^2}{e^{\frac{F}{\lvert\mathcal{F}_s\rvert}}}$	$\lvert\mathcal{F}_s\rvert x$	Yes	Yes

The in-line and in-space neighboring matrices of the first B-PLC test network are as below and its other details are provided in Table 2.

$$M^{NB_L} = \begin{bmatrix} 0 & 1 & 0 \\ 1 & 0 & 1 \\ 0 & 1 & 0 \end{bmatrix}, \quad M^{NB_S} = \begin{bmatrix} 0 & 0.2 & 0 \\ 0.5 & 0 & 0.1 \\ 0 & o.3 & 0 \end{bmatrix} \tag{3}$$

Table 2: Specifications of the first B-PLC test network

$\lvert\mathcal{C}\rvert = 3,\ \lvert\mathcal{F}_s\rvert = 10$		
$\mathcal{C}_i$	$\lvert F^i_{Req}\rvert$	$\boldsymbol{\mathcal{F}}^i_{Forbid}$
$\mathcal{C}_1$	5	$\{9,10\}$
$\mathcal{C}_2$	5	$\{2,3\}$
$\mathcal{C}_3$	6	$\{5,10\}$

As can be seen from the Table 2, this test network totally needs 16 frequencies and the PLC-CA solution must assign them from the available ten frequencies by taking the forbidden sets and neighboring model into account. In the other words, the solution matrix $\boldsymbol{M}^{CA}$ must such that while the assigned frequency sets to the cells, i.e. $\mathcal{F}^i_{CA}$, belonging to their allowable frequency sets $\mathcal{F}^i = \mathcal{F}_s - \mathcal{F}^i_{Forbid}$, the frequencies of the neighbor cells be far away from each other's as much as possible.

For the numerical simulations, a random population of size $N = 40$ is first generated for both GA and SFLA, and fitness value for the elements of this population are calculated according to the network's interference given in (2). Then, for the GA, the members (chromosomes) of this population exchanged their information through GA operations including elitism, selection, crossover of rate 0.9 and mutation of rate 0.1, to produce next generation of chromosomes and this process is continued until an optimal solution is obtained or stopping criterion is met. For the SFLA, the generated random population is subdivided into $m = 10$ memeplexes, each contains $n = N/m = 4$ members (frogs). Then, a local search is performed for each memeplex to improve the frog with the worst fitness. When tenth iterations of local search are performed, all frogs of population are mixed together and partitioned into $m = 10$ memeplexes again to repeat the local search. This process is continued iteration by iteration until an optimal solution is obtained or stopping criterion is met.

In the cases of first B-PLC test network, the curves of the best fitness (co-site interference) versus iteration (for both GA and SFLA) have been depicted in Fig. 3 for the first scenario and Fig. 4 for the second one.

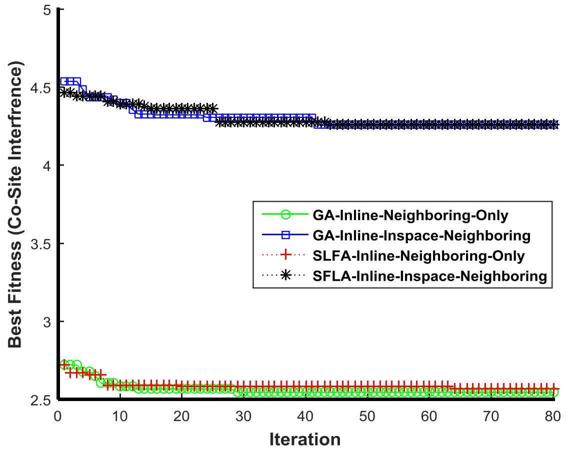

Fig. 3: First B-PLC test network: curves of the co-site interference versus iterations for the first scenario.

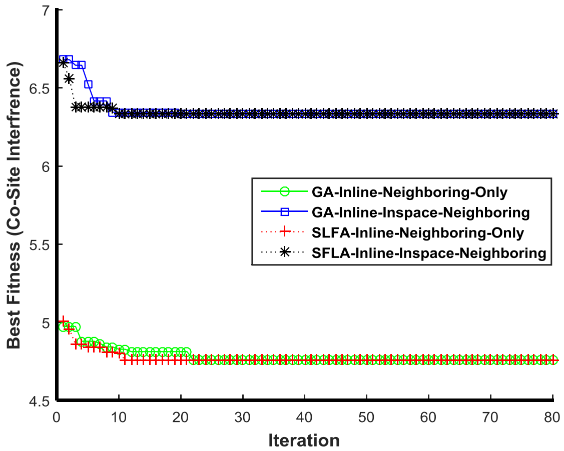

Fig. 4: First B-PLC test network: curves of the co-site interference versus iterations for the second scenario.

Further, the solution matrix of the first scenario takes one of the following forms for each realization of GA and SFLA:

$$\boldsymbol{M}^{CA} = \left\{ \begin{array}{l} \begin{bmatrix} 1 & 1 & 1 & 1 & 1 & 0 & 0 & 0 & 0 & 0 \\ 0 & 0 & 0 & 0 & 0 & 1 & 1 & 1 & 1 & 1 \\ 1 & 1 & 1 & 1 & 1 & 1 & 0 & 0 & 0 & 0 \end{bmatrix} \\ \begin{bmatrix} 0 & 0 & 0 & 0 & 0 & 1 & 1 & 1 & 1 & 1 \\ 1 & 1 & 1 & 1 & 1 & 0 & 0 & 0 & 0 & 0 \\ 0 & 0 & 0 & 0 & 1 & 1 & 1 & 1 & 1 & 1 \end{bmatrix} \end{array} \right. \quad (4)$$

However, in the case of the second scenario, the solution matrix has only below format:

$$\boldsymbol{M}^{CA} = \begin{bmatrix} 1 & 1 & 1 & 1 & 1 & 0 & 0 & 0 & 0 & 0 \\ 0 & 0 & 0 & 0 & 0 & 1 & 1 & 1 & 1 & 1 \\ 1 & 1 & 1 & 1 & 0 & 1 & 1 & 0 & 0 & 0 \end{bmatrix} \quad (5)$$

As demonstrated in Fig. 3 and Fig. 4, the suggested interference function can successfully model and track the network interference according to the considered neighboring schemes in the two considered cases for each scenario. Moreover, as evident from (4) and (5), the resulting solution matrices indicating to an optimum channel allocation for the both scenarios and also for both GA and SFLA. This is because the assigned frequency sets to the neighboring cells have the maximum distance from each other's. Expressing in details, these results and their modifications with respect to existing studies can be highlighted as below:

- First, since the case 1 of each scenario only considers in-line neighboring scheme and in case 2 both in-line and in-space neighboring are taken into account, these two cases compare the results of our suggested model for PLC-CA problem in which co-site interference varies depending on neighboring intensity and assigned frequency sets to the cells with that one in which interference variations is only due to changes in assigned frequency sets. Due to taking both in-line and in-space neighboring schemes into account for the actual B-PLC networks of the case 2, it is evident that the amount of co-site interference imposed on this real network must be more than of case 1. As shown in Fig. 3 and Fig. 4, the suggested interference function of (2) can properly model and successfully track the variations of co-site interference in these two cases. Noted that the case 1 of each scenario can be considered as an improved version of the assumed model in [23]-[25]. This is due to the fact both ones, i.e. case 1 and the works of [23]-[25], relying on in-line neighboring scheme; However, the co-site interference of case 1 varies according to the distance between assigned frequency sets, but this dependency has not considered in [23]-[25]. Thus, the results of the cases 1 and 2 provide a comparison between the results of previous studies and our method.
- Second, both GA and SFLA leading to optimum channel allocation for all considered cases and scenarios. For instance, as evident from (4) and (5), there is no common frequencies between assigned sets to the cells 1 and 2 of the first test network. Note that existence of one common frequency for cells 2 and 3 of (4) is due to the fact that these two cells totally needing 11 frequencies, this is while the available OFDM channels are equal to $|\mathcal{F}_s| = 10$. Similarly, existence of two common frequencies for

these cells in (5) is due to limited number of OFDM channels and also due to considering forbidden sets which restricts it more cells. It is also important to be noted that when the solution matrices are compered for two different pairs of neighbor cells at intermediates iterations, it is observed that distance between assigned frequency sets to cells of pair with greater neighboring intensity is more than that of other pair. This is due to the fact that we defined the interference distance matrix so that the considered solver be more sensitive to the cells having greater neighboring intensity and as a result, the frequencies allocated to these cells have more distance from each other in intermediates steps where the optimal solution for the network has not been obtained yet.

- Third, as demonstrated in Fig. 3 and Fig. 4, both GA and SFLA are finally converged to a similar co-site interference. However, they reach to this value in different iterations due to difference in computational complexity. Expressing more precisely, if the solution matrix of the GA and SFLA, i.e. $\boldsymbol{M}^{CA}$, is compared before convergence at an intermediate iteration, it is observed that SFLA providing a more optimal solution than the GA. However, it should be noted that this comparing is not entirely accurate because SLFA also benefits from an iteration-based local search in each iteration. Therefore, it can be concluded that the SFLA provides better solutions in intermediate iterations due to performing local search and wasting the time; however, the both ones eventually leading to an optimal solution.
- Forth, curves of co-site interference versus iterations have an expected behavior for both GA and SFLA and follows a non-increasing function. Further, when forbidden sets of the frequencies are considered in the second scenario of Table 1, both GA and SFLA successfully avoids assignment of these sets to the B-PLC cells and the channels are allocated according to the allowable frequency sets $\mathcal{F}^i = \mathcal{F}_s - \mathcal{F}^i_{Forbid}$.
- Eventually, the comprehensiveness of the suggested interference function is also confirmed by performing numerical simulations for two different realizations of both $G_1(F, x)$ and $G_2(x)$. Note that these functions are utilized in (1) and (2) to define co-site interference.

Here, the second test network is considered to evaluate performances of the suggested model for a more complex structure. Notes this network is consisted of the six B-PLC cells and exploits OFDM modulation of $|\mathcal{F}_s| = 64$ frequencies.

The other details of this network are provided in Table 3 and its in-line and in-space neighboring matrices are given in (6) and (7).

$$\boldsymbol{M}^{NB_L} = \begin{bmatrix} 0 & 0 & 0 & 1 & 0 & 0 \\ 0 & 0 & 0 & 0 & 0 & 0 \\ 0 & 0 & 0 & 0 & 0 & 0 \\ 1 & 0 & 0 & 0 & 0 & 0 \\ 0 & 0 & 0 & 0 & 0 & 1 \\ 0 & 0 & 0 & 0 & 1 & 0 \end{bmatrix}, \tag{6}$$

$$\boldsymbol{M}^{NB_S} = \begin{bmatrix} 0 & 0 & 0 & 0.9 & 0 & 0 \\ 0 & 0 & 0.7 & 0 & 0 & 0 \\ 0 & 0.7 & 0 & 0 & 0 & 0 \\ 0.9 & 0 & 0 & 0 & 0 & 0 \\ 0 & 0 & 0 & 0 & 0 & 0 \\ 0 & 0 & 0 & 0 & 0 & 0 \end{bmatrix} \tag{7}$$

Table 3: Specifications of the second B-PLC test network

$\|\mathcal{C}\| = 6,\ \|\mathcal{F}_s\| = 64$		
$\mathcal{C}_i$	$\|F^i_{Req}\|$	$\boldsymbol{\mathcal{F}^i_{Forbid}}$
$\mathcal{C}_1$	20	{61,62,63,64}
$\mathcal{C}_2$	15	{1,2, 3, 4, 5}
$\mathcal{C}_3$	32	∅
$\mathcal{C}_4$	40	∅
$\mathcal{C}_5$	27	{1, 2, 10, 44 ,45}
$\mathcal{C}_6$	27	{60, 61,62,63,64}

For the numerical simulations of the second B-PLC test network, population size has been considered equal to $N = 120$ and crossover and mutation rates of the GA are set to 0.9 and 0.2, respectively. For the SFLA, this population is subdivided into $m = 12$ memeplexes of $n = N/m = 10$ members. Curves of the best fitness versus iterations have been depicted in Fig. 5 for the first scenario and Fig. 6 for the second one.

Furthermore, according to the solution matrix of the first scenario, the assigned sets to the neighboring cells 1 and 4 have one of the following forms:

$$\begin{cases} \mathcal{F}^1_{CA} = \{1,2, \dots ,20\}, \mathcal{F}^4_{CA} = \{64,63, \dots ,25\} \\ \mathcal{F}^1_{CA} = \{64,63, \dots ,45\}, \mathcal{F}^4_{CA} = \{1,2, \dots ,40\} \end{cases} \tag{8}$$

However, when the forbidden sets are taken into the account for the second scenario, the solution is:

$$\mathcal{F}^1_{CA} = \{1,2, \dots ,20\}, \mathcal{F}^4_{CA} = \{64,63, \dots ,25\} \tag{9}$$

In similar manner, for the first scenario, the assigned sets to the neighboring cells of 5 and 6 belonging to one of the following groups:

$$\begin{cases} \mathcal{F}^5_{CA} = \{1, \dots ,27\}, \mathcal{F}^6_{CA} = \{64, \dots ,38\} \\ \mathcal{F}^5_{CA} = \{64, \dots ,38\}, \mathcal{F}^6_{CA} = \{1, \dots ,27\} \end{cases} \tag{10}$$

However, due to considering forbidden sets in the second scenario, the solution will be as:

$$\begin{cases} \mathcal{F}^5_{CA} = \{64,63, \dots ,46,43,42, \dots ,36\} \\ \qquad \mathcal{F}^6_{CA} = \{1, \dots ,27\} \end{cases} \tag{11}$$

As can be seen from Fig. 5 and Fig. 6, the curves of the co-site interference have their expected behavior as non-increasing functions and track the network interference according to the considered cases in these scenarios. Furthermore, as evident from (8)-(11), there is no common frequencies between assigned sets to the neighboring cells, i.e. cells 1 and 4, and cells 5 and 6. Moreover, the assigned sets to these cells have maximum distance from each other. In general, it is observed that the numerical results of the second test network are consistent with that one of the first test network and all mentioned points for the results of first test network are valid for the second one as well. Thereby, it is concluded that the suggested method has the ability to model PLC-CA problem in actual scenarios, tracking the network interference in these situations and providing an optimal solution for them. Further, it is confirmed the suggested method, as a comprehensive model, includes all previous research.

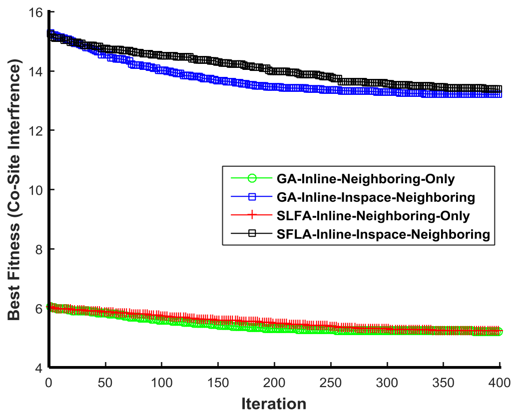

Fig. 5: Second B-PLC test network: curves of the co-site interference versus iterations for the first scenario.

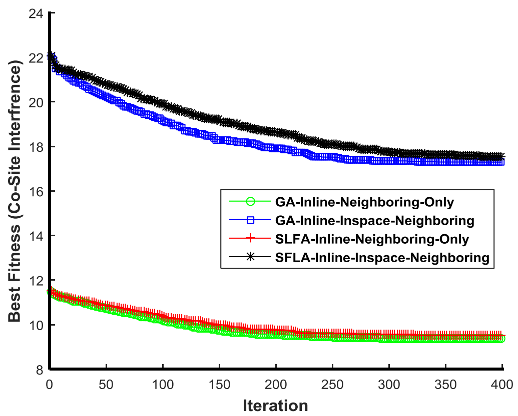

Fig 6: Second B-PLC test network: curves of the co-site interference versus iterations for the second scenario.

Conclusion

In this paper, the problem of channel allocation was investigated for the B-PLC access network. In order to overcome the limitations of the existing study and provide a comprehensive analysis, an actual B-PLC access that is in expose of both in-line and in-space neighboring schemes was assumed and the problem modelling, formulations, and suggested solutions are planned in this regard. To achieve these goals, PLC-CA problem is first formalized as an optimization problem; in-line neighboring is considered as zero number or one; in-space neighboring is modeled as a real number from the interval [0 1]; and the aggregate neighboring intensity is assumed as the summation of these two numbers. Then, the co-site interference of the B-PLC access networks is defined as a function of the aggregate neighboring intensity and the assigned frequency sets to the cells, so that when the value of neighboring intensity is increased and the distance of assigned frequency sets is decreased, the interference is increased. Finally, the meta-heuristic methods of GA and SFLA were employed to solve the resulting PLC-CA problem and evaluate its performance for different scenarios and compare it with the existing research. The results were confirmed that suggested method can successfully model channel allocation problem in actual B-PLC networks and provides an optimum solution for both GA and SFLA by avoiding the assignment of forbidden frequencies and increasing the distance between neighboring cells as much as possible. It was also revealed that this method includes and improves all previous research and worked as a comprehensive alternative for tracking co-site interference in different situations.

Author Contributions

M. Sheikh-Hosseini designed and modeled the suggested methods for the PLC-CA problem and wrote the manuscript.

S. M. Nosratabadi designed the experiments and edited the manuscript.

Acknowledgment

The authors would like to acknowledge the financial support of Institute of Science and High Technology and Environmental Sciences, Graduate University of Advanced Technology, Kerman, Iran, under Contract number 96/3166.

Conflict of Interest

The authors declare no potential conflict of interest regarding the publication of this work. In addition, the ethical issues including plagiarism, informed consent, misconduct, data fabrication and, or falsification, double publication and, or submission, and redundancy have been completely witnessed by the authors.

Abbreviations

PLC	Power Line Communications
B-PLC	Broadband-PLC
N-PLC	narrowband-PLC
PLC-CA	PLC Channel Allocation
BS	Base Station

GBSP	Generalized Base Station Placement
GA	Genetic Algorithm
SFLA	Shuffled Frog-Leaping Algorithm
OFDM	Orthogonal Frequency Division Multiplexing

References

[1] M. Schwartz, "Carrier-wave telephony over power lines: Early history," IEEE Commun. Mag., 47(1): 14-18, 2009.

[2] S. Mudriievskyi, "Power line communications: State of the art in research, development and application," AEU Int. J. Electron. Commun., 68(7): 575-577, 2014.

[3] C. Cano et al., "State of the art in power line communications: From the applications to the medium," IEEE J. Sel. Areas Commun.," 34(7): 1935-1952, 2016.

[4] S. Galli, A. Scaglione, Z. Wang, "For the grid and through the grid: the role of power line communications in the smart grid," Proc. IEEE, 99(6): 998-1027, 2011.

[5] M. Sheikh-Hosseini, "Evolution of power line communications: From a fixed telephone system to telecommunication technology of smart energy grid," Ir Iran. J. Eng. Educ., 20(80): 71-96, 2019.

[6] S. Chen et al., "Ultra-Wideband Powerline Communication (PLC) above 30MHz," IET Commun., 3(10): 1587-1596, 2009.

[7] K. Ramanathan, N.J.R. Muniraj, "DWT-IDWT-based MB-OFDM UWB with digital down converter and digital up converter for power line communication in the frequency band of 50 to 578 MHz," Ann. Telecommun., 70: 181-196, 2015.

[8] M. Sheikh-Hosseini, G.A. Hodtani, M. Molavi-kakhki, "Capacity analysis of PLC point-to-point and relay channels," Trans. Emerging Telecommun. Technol., 27(2): 200-215, 2016.

[9] L. Lampe, A.M. Tonello, T.G. Swart, Power Line Communications: Principles, Standards and Applications from multimedia to smart grid. John Wiley & Sons, 2016.

[10] E. Ancillotti, R. Bruno, M. Conti, "The role of communication systems in smart grids: Architectures, technical solutions and research challenges," Comput. Networks, 36(17): 1665–1697, 2013.

[11] A. Pittolo et al., "In-vehicle power line communication: Differences and similarities among the in-car and the in-ship scenarios," IEEE Veh. Technol. Mag., 11(2): 43-51, 2016.

[12] M Yigit et al., "Power line communication technologies for smart grid applications: A review of advances and challenges," Comput. Networks, 70: 366-383, 2014.

[13] G. Lopez et al., "The role of power line communications in the smart grid revisited: Applications, challenges, and research initiatives," IEEE Access, 7: 117346-117368, 2019.

[14] M. Kashef, M. Abdallah, M.N. Al-Dhahir, "Transmit power optimization for a hybrid PLC/VLC/RF communication system," IEEE Trans. Green Commun. Networking, 2(1): 234-245, 2017.

[15] Y.S. Reddy et al., "Optimisation of indoor hybrid PLC/VLC/RF communication systems," IET Commun., 14(1): 117-126, 2020.

[16] M. Sheikh-Hosseini, G.A Hodtani, "On the capacity of additive white mixture gaussian noise channels," Trans. Emerging Telecommun. Technol., 30(7): e3585, 2019.

[17] E. Biglieri, "Coding and modulation for a horrible channel," IEEE Commun. Mag., 41(5): 92-98, 2003.

[18] M. B. Noori Shirazi, A. Golestani, H. Ahmadian Yazdi, A. Habibi Daronkola, "Analysis and comparison of PAPR reduction techniques in OFDM systems," J. Electr. Comput. Eng. Innovations, 3(1): 37-45, 2015.

[19] A. Haidine, I. Mellado, R. Lehnert, "PANDeMOO: Powerline communications access network designer based on multi-objective optimisation," presented at the IEEE Symp. ISPLC, Vancouver, Canada, 2005.

[20] A. Haidine, R. Lehnert, "Solving the generalized base station placement problem in the planning of broadband power line communications access networks," presented at the 2th IEEE Conf. AccessNets., Ottawa, Ont., Canada, 2007.

[21] A. Haidine, R. Lehnert, "Placement of base stations in broadband power line communications access networks by means of multi-criteria optimization," presented at the 3th IEEE Conf. AccessNets., Las Vegas, USA, 2008.

[22] A. Haidine, R. Lehnert, "Optimisation of base station location in broadband power line communications access networks," Int. J. Comm. Network Distr. Syst., 5(4): 347-374, 2010.

[23] A. Haidine, R. Lehnert, "Analysis of the channel allocation problem in broadband power line communications access network," presented at the IEEE Symp. ISPLC, Pisa, Italy, 2007.

[24] A. Haidine, R. Lehnert, "Modeling of channel allocation in broadband powerline communications access networks as a multi-criteria optimization problem," presented at the 3th IEEE Conf. AccessNets., Las Vegas, USA, 2008.

[25] A. Haidine, R. Lehnert, "The channel allocation problem in broadband power line communications access networks: analysis, modeling and solutions," Int. J. Autonom. Adapt. Comm. Syst., 3(4): 396-418, 2010.

[26] L.P. Do, R. Lehnert, "Dynamic resource allocation protocol for large PLC networks," presented at the IEEE Symp. ISPLC, Beijing, China, 2012.

[27] R. Kulshrestha, "Channel allocation and ultra-reliable communication in CRNs with heterogeneous traffic and retrials: A dependability theory-based analysis," Comput. Commun., 158: 51-63, 2020.

[28] H. Zhang, H. Li, J.H. Lee, "Efficient subchannel allocation based on clustered interference alignment in ultra-dense femtocell networks," China Commun., 14(4): 1-10, 2017.

[29] M.H. Refan, A. Dameshghi, "RTDGPS implementation by online prediction of GPS position components error using GA-ANN model," J. Electr. Comput. Eng. Innovations, 1(1): 43-50, 2013.

[30] Y. Rohani, Z. Torabi, S. Kianian, "A novel hybrid genetic algorithm to predict students' academic performance," J. Electr. Comput. Eng. Innovations, 8(2): 219-232, 2020.

[31] T.H. Huynhm "A modified shuffled frog leaping algorithm for optimal tuning of multivariable PID controllers," in Proc. 2008 IEEE International Conference on Industrial Technology: 1-6, 2008.

Biographies

Mohsen Sheikh-Hosseini was born was born in Iran in 1983. He received the B.S. degree in electrical engineering from Shahid Bahonar University of Kerman, Kerman, Iran in 2007, and then he received the M.S. and Ph.D. degrees both in telecommunications from Ferdowsi University of Mashhad, Mashhad, Iran in 2009 and 2014, respectively. He is currently with the Department of Computer and Information Technology, Institute of Science and High Technology and Environmental Sciences, Graduate University of Advanced Technology, Kerman, Iran. His research interests include wireless communications, power line communications, wireless sensor networks, smart grids, and machine learning applications in telecommunications.

Seyyed Mostafa Nosratabadi received the B.Sc. degree from Shahid Bahonar University of Kerman, Kerman in 2008, M.Sc. degree from University of Kashan in 2011, both in electrical engineering. He received Ph.D. degree in electronics engineering from university of Isfahan, Iran, in 2016 and then joined to Department of Electrical Engineering, Sirjan University of Technology, Sirjan. His research interests are analysis of power systems, power electronic, smart grid and micro grid.

How to cite this paper:
M. Sheikh-Hosseini, S.M. Nosratabadi, "Modelling and optimization of channel allocation for power line communications access networks in the presence of in-line and in-space interference," J. Electr. Comput. Eng. Innovations, 9(1): 103-114, 2021.

DOI: 10.22061/JECEI.2020.7459.395

URL: http://jecei.sru.ac.ir/article_1491.html